Journal of Advanced Research Design 138, Issue 1 (2026) 116-128

Penerbit Akademia Baru

Journal of Advanced Research Design

Journal homepage:
https://akademiabaru.com/submit/index.php/ard
ISSN: 2289-7984

Modelling Plant Stress in Mature Oil Palm for Basal Stem Rot Disease Severity with Water Use Efficiency and Hyperspectral Data

Mohd Sharul Aikal Baharim[1], Nor Aizam Adnan[2,*], Angelynna Lovelyn Laurence[2], Mohamad Izzuddin Anuar[3], N. Nurhamidah[4]

[1] Department of Survey and Mapping Malaysia, Cartography and GIS Division, 50578 Kuala Lumpur, Wilayah Persekutuan Kuala Lumpur, Malaysia
[2] Surveying Science and Geomatics, Faculty of Built Environment, Universiti Teknologi MARA, 40450 Shah Alam, Selangor, Malaysia
[3] Malaysian Palm Oil Board, Bandar Baru Bangi, 43000 Kajang, Selangor, Malaysia
[4] Department of Civil Engineering, Faculty of Engineering, Andalas University, Limau Manis, Padang West Sumatra, 25163, Indonesia

ARTICLE INFO

Article history:
Received 21 February 2025
Received in revised form 14 March 2025
Accepted 30 June 2025
Available online 20 July 2025

Keywords:
Ganoderma basal stem rot; hyperspectral data; UAV; WUE; stepwise modelling; oil palm

ABSTRACT

The Basal Stem Rot (BSR) disease brought by the *Ganoderma Boninense* pathogen is regarded as a huge killer for oil palm producers' countries, particularly Malaysia and Indonesia oil palm plantations. Various methods are being deployed for assessment of the disease, especially in the early phase however not yield satisfactory results. Therefore, this research study tends to predict plant stress affected by BSR disease infection with plant physiology variables specific to water use efficiency (WUE) with hyperspectral data in oil palm to provide a better assessment of BSR disease The objective of this research is to develop a new model in plant stress with WUE variable and hyperspectral data in oil palm tree. Second, to assess mapping for estimation of oil palm trees in plantation. Based on the result obtained, 4 models established show a significant result based on training and validation samples in RMSE, and regression plot values were sorted by rank (Model 1, Model 2, Model 4, and Model 3). In mapping analysis, it highlighted the distance between affected oil palm trees might influence the WUE estimation and the addition of hyperspectral data improved the visualization in the map generated from the model

1. Introduction

In the food business, palm oil is frequently regarded as a significant vegetable oil for consumers [1]. The oil palm industry has a significant economic impact on the major palm oil producers, such as Malaysia and Indonesia. Records show that Sumatra, Indonesia was the first location in Southeast Asia to produce the oil palm tree (*Elaeis guineensis Jacq.*). According to Murphy *et al.,* [2], they claimed that Malaysia is adopting the strategy and encouraging effective oil palm development and diversification by imitating Indonesia. The industry's requirement for oleochemicals and bioenergy, among other factors, caused crude palm oil prices to increase significantly. Among these factors were the industrial requirements for bioenergy and oleochemicals. These driving forces have been a major

* *Corresponding author*
E-mail address: nor_aizam@uitm.edu.my

https://doi.org/10.37934/ard.138.1.116128

part of the palm oil industry's expansion in recent decades, and it is anticipated that the demand for palm oil will continue to rise. The aforementioned scenario represents a positive development for oil palm-producing countries, but if a plant disease called Basal Stem Rot (BSR) disease persists in attacking oil palm plantations and reducing oil palm productivity, it could have a substantial negative impact on the sustainability of oil palm.

Oil palm trees are frequently affected by a deadly plant disease called BSR disease. The BSR disease is caused by the plant pathogen Ganoderma, which has a major impact on the oil palm plantation industry's production and economy. According to Jazuli *et al.,* [3], it has been indicated that almost 60% of the nation's oil palm crops have been affected by BSR disease, which was disseminated by a white-rot fungus related to the Ganoderma spp. families. Specifically, it has been documented that at least seven distinct species of the Ganoderma pathogen (*G. Boninense, G. Miniatocinctum Steyaert, G. Chalceum (Cooke) Steyaert, G. Tornatum (Pers.) Bers., G. Xylonoides Steyaert*, and *G. Ryvard*) can be found in Malaysia, Indonesia, Papua New Guinea and Cameroon. Through research conducted by Paterson [4], regardless of the history of the crops when they were disease-free, the BSR disease was gradually shown to be in superficial condition at high levels in oil palms in inland lateritic soils and peat soils. It had been assumed that older palm trees between the ages of 25 and 30 were more susceptible to BSR disease. According to Zakaria [5], once the symptoms develop, the diseased trees may die between 6 to 24 months for young palms and one to two years for senior palms. Ultimately, to extend the life of damaged oil palms, Siddiqui *et al.,* [6] stated that the farmers must keep treating the plantation with biological control agents. Currently, various techniques and methods have been developed for the assessment of the BSR disease including destructive (cutting the trees) or non-destructive methods (remote sensing, tomography, e-nose application, dielectric properties, etc.) for early assessment of BSR disease yet none of these shows an absolute solution for the issue [7,8]. Therefore, this study tends to predict a plant stress affected by BSR disease infection with plant physiology variables specific water use efficiency (WUE) with hyperspectral data in oil palm tree with leaf physiology variable specific WUE with airborne hyperspectral data for better assessment in early evaluation of the disease [9]. The research objectives involved developing a new novelty model of WUE for estimation and assessment of the map generated by the model.

2. Methodology

2.1 Ground Census Data

The ground census data were rigorously collected on-site at the Felcra Lekir Oil Palm Plantation in Perak, Malaysia with accurate latitude and longitude coordinates of 4°11'51.89''N and 100°47'11.92''E. The data was collected on 6/3/2023 to support the analysis and assisted by the BSR disease team of experts from the Malaysian Palm Oil Board (MPOB) by following standard BSR severity levels guidelines as shown in Table 1.

Table 1
BSR disease severity guidelines by MPOB

BSR Disease Severity	Infection Level	Description
T0	Healthy	No infection/No fruiting body *G.Boninense*, no foliar symptoms or stem rotting at the base
T1	Early	Presence of white mycelium or fruiting body *G.Boninense* without foliar symptoms or stem rotting <10%
T2	Moderate	The presence of white mycelium or fruiting body *G.Boninense*. Foliar symptoms: Bending crown more than 50%, some frond yellowing. Stem rotting <30%
T3	High	The presence of white mycelium or fruiting body *G.Boninense*. Foliar symptoms: Bending crown more than 50%, some frond yellowing and brown. Stem rotting >30% or appear a big hole at the base trunk.
T4	Severe	Oil palm collapsed

Figure 1 depicts the sample of trees in the oil palm plantation according to the BSR disease severity levels for healthy (T0) and non-healthy trees (T1, T2, T3).

Fig. 1. Oil palm tree condition in BSR disease severity

2.2 Leaf Physiology Data

In leaf physiology data collection, the sample trees being chosen consisted of four levels of BSR disease severity (T0, T1, T2, and T3) with (T0- 6 Tree, T1- 6 Tree, T2- 6 Tree, T3- 6 Tree). This amounted to a total of 24 trees for oil palm tree samples. Two frond numbers were chosen (frond 9 and frond 17) for WUE measurement with other variables in response to BSR disease severity due to the limitation of time. In the leaflets sample from both frond numbers, only six (6) leaflets were selected from the whole leaflets. The leaflet samples were obtained from fronds started from the rachis part as recommended by the MPOB guidelines. Leaflet samples measured leaf physiology parameters which consisting of Photosynthetic Rate (P_r), Transpiration Rate (T_r), Temperature Leaf (TempL), Intercellular CO_2 Concentration (Ci), and Stomatal Conductance (g_s) using two portable equipment sensors of the photosynthesis system (LI-6400XT, LiCOR Inc., USA) while the leaflet was still intact with the frond sample for both fronds number The condition of the inside of the leaf curvette for LiCOR was as follows: ambient humidity, ambient temperature, photosynthetically active (PAR) with 1000 photon µmol m^{-2} s^{-1} (red/blue light) and reference CO2 of 400 µmol mol^{-1}. Meanwhile, the main parameter in this study involved the calculation of the instantaneous WUE (E) variables using the formula WUE = (P_r/T_r) as the WUE variable does not provide directly from the instrument as applied by A'fifah *et al.,* [10]. The data measurement was conducted during the photosynthesis period between 8.00 and 11.30 a.m. similar to Koyama *et al.,* [11]. All the data variables collected were automatically stored in LiCOR and downloaded for further analysis. Additionally, a portable SPAD 502 equipment was used to apply the SPAD (Soil Plant Analysis Development) method to determine the leaflets' relative chlorophyll content (F) where three different points (left, centre, and right) on both sides were used to measure the leaflets.

2.3 Airborne Hyperspectral Data

In the next phase, it's continued with airborne hyperspectral image data collection for oil palm plantations on the same date. The hyperspectral Resonon Pika L sensor mounted on a DJI Matrice 600 Pro drone has been utilized to cover the study area in an oil palm plantation by an MPOB expertise pilot drone. The hyperspectral image data collection was simultaneously conducted with leaf physiology measurement (LiCOR and SPAD). The details of flight planning and airborne specification are revealed in Table 2 and Figure 2.

Table 2
Details of flight planning in hyperspectral image data collection

Scanned Method	Push Broom Scanner
Scanned Line	37 lines
Overlaps Scanline	Front and Side overlaps ratio: 10%, 90%
Altitude	90 meters above ground
Speed	7.7 m/s
Camera Shutter Interval	10.5 sec
Flying Time	8.00 a.m – 11.00 a.m

Airborne Specification

Sensor Brand: Hyperspectral Resonon Pika L
Drone Brand: DJI Matrice 600 Pro
Spectra Range: 400 – 1000
Band Range: 300
Spectral Resolution (nm): 2.7
Spatial Pixels: 900
Bit: 16 Bit
Max Frame Rate (fps): 249
Weight without lens (Kg): 0.64

Fig. 2. Hyperspectral drone sensor with their specification

2.4 Hyperspectral Image Processing

The hyperspectral data images are being processed with a few methods in enhancement and transformation such as Savitzky-Golay, 1st derivative, and Continuum Removal (CR). These methods have been chosen as highly recommended to improve the quality of the images captured and assist in feature detection by several authors [10-12]. The formulas used for Savitzky-Golay, 1st derivative, and Continuum removal techniques are shown in Eqs. (1) to (5) as below:

Savitzky-Golay Technique

$$y_K = \frac{\sum_{i=-m}^{i=m} C_i \text{x}\, C_{k+i}}{N} \tag{1}$$

where: y = original image spectral value
y_K = Filtered image spectral value
C_i = Coefficient of the i^{th} spectral value of the filter (smoothing window)
N = Number of convolutions integer equal to smoothing window size (2m +1)

1st derivative Technique:

$$\frac{\partial \mathrm{f(x,y)}}{\partial \mathrm{x}} = \Delta\mathrm{x} = \frac{\mathrm{f(x+dx,y)-f(x,y)}}{\mathrm{dx}} \tag{2}$$

$$\frac{\partial \mathrm{f(x,y)}}{\partial \mathrm{y}} = \Delta\mathrm{y} = \frac{\mathrm{f(x,y+dy)-f(x,y)}}{\mathrm{dy}} \tag{3}$$

$$\Delta x = f\ (i{+}1, j) - f\ (i, j),\ \boldsymbol{\Delta} y = f\ (i, j{+}1) - f\ (i, j) \tag{4}$$

where: dx, dy = Number of pixels between 2 points
$(i\ , j)$ = Point pixel of image coordinates (dx = dy =1 : pixel spacing)
Δx, Δy = Intensity gradient of the image

Continuum Removal (CR)

$$\mathrm{CRR} = \frac{\mathrm{R}}{\mathrm{CR}} \tag{5}$$

where: CRR = Continuum-removed reflectance
R = Original Reflectance
C = Continuum curve

The image processing process continued with the extraction process of spectral data and was subjected to meticulous processing using advanced remote sensing software, notably ENVI Classic software. The process started by extracting the spectral data using the tool Spectrum Profile in the software for the above crown canopy trees of the selected sample trees (24 samples) for an image produced and determined for significant hyperspectral wavelength in MATLAB software through feature selection of Minimum Redundancy Maximum Relevance (MRMR) in Support Vector Machine (SVM) classification as applied by many authors [12-18].

2.5 WUE Hyperspectral Modelling in Stepwise Multiple Linear Regression Model

In the modelling phase, stepwise multiple linear regression modelling has been chosen widely in model development as a popular data-mining tool that uses statistical significance to select the explanatory variables to be used as stated by Ali *et al.,* [19]. In terms of the cross-validation model, the sample (training model:70%, validation model:30%) has been applied for the model development for a better assessment of model reliability similar to Viertel *et al.,* [20]. In the end, the accuracy assessment was measured by comparing the forecasted model with actual data in Root Mean Square Error (RMSE) and regression plot value [21].

2.6 Mapping WUE Hyperspectral Modelling

In the final phase, all significant leaf physiology is converted into geospatial data using Inverse Distance Weightage (IDW) in order to align the format in map-produced estimation as well as in the WUE variable as recommended by Li [22]. In the end, together with a significant hyperspectral wavelength image, all the models are mapped for the mapping assessment.

3. Results

Figure 3 shows the distribution of the sample collected in the oil palm Felcra Lekir plantation where the sample is T0: 6 trees, T1: 6 trees, T2: 6 trees, and T3: 6 trees. This accumulated 24 sample trees measured for analysis and model development.

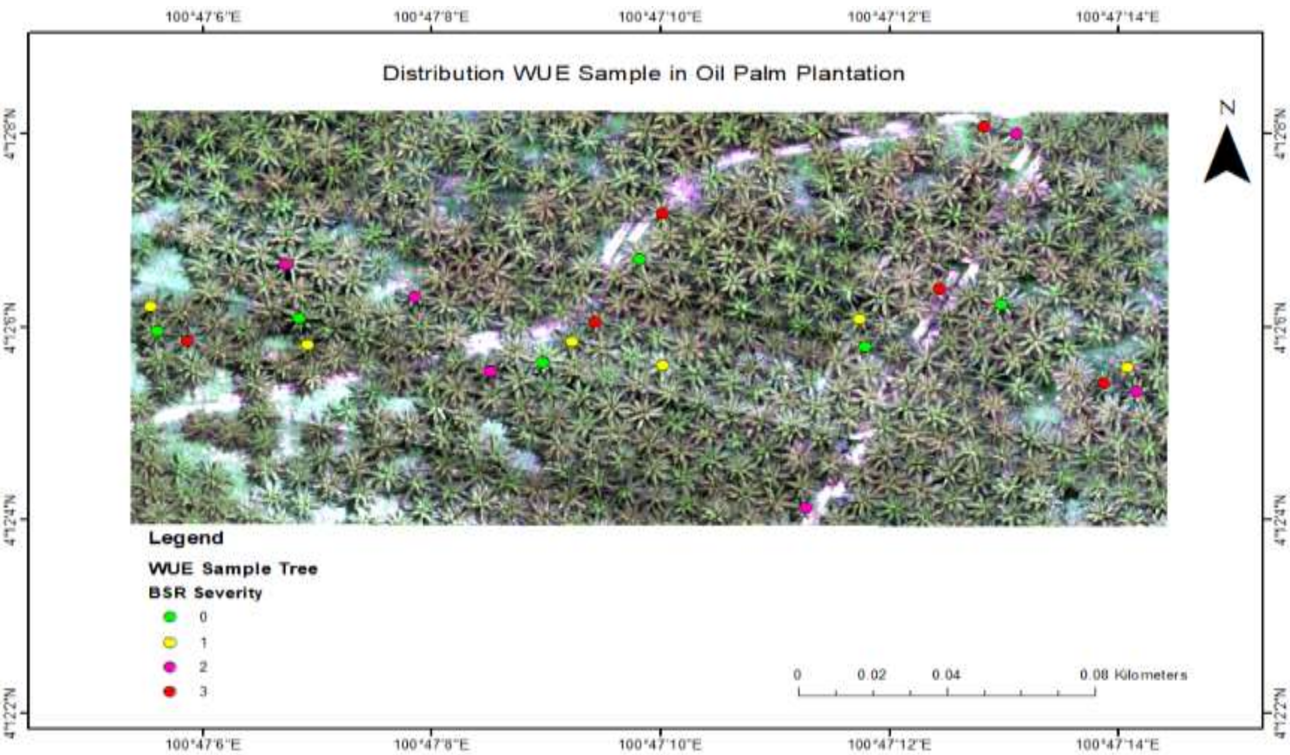

Fig. 3. Distribution of BSR disease severity samples in oil palm on plantation

Figure 4 shows the hyperspectral image map that has been generated after image processing through image enhancement and transformation (Savitzky-Golay, 1st derivative, and Continuum Removal (CR) techniques) for WUE hyperspectral modelling. Through SVM classification in MATLAB software, 5 significant wavelengths have been identified for model development including w717.4, w736.7, w741, w790.8, and w860.7.

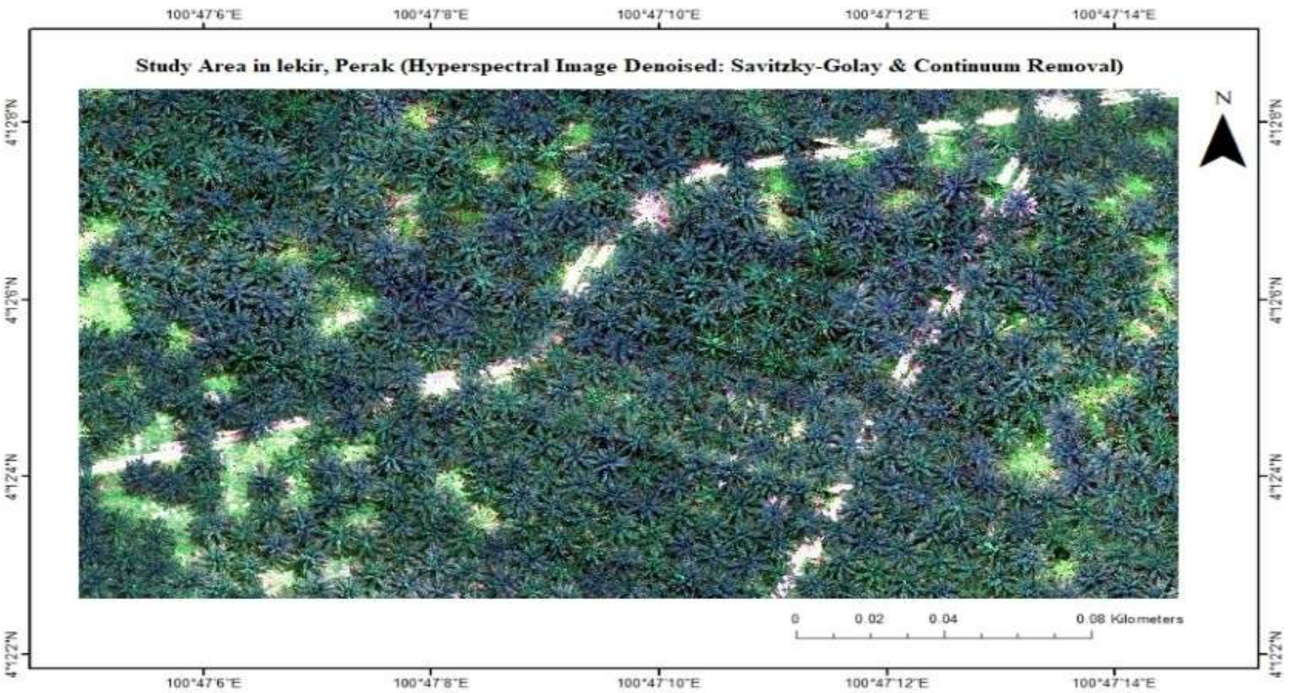

Fig. 4. Oil palm plantation hyperspectral image with enhancement and transformation (Savitzky-Golay, 1st derivative and CR techniques)

3.1 Evaluation Forecast Modelling Hyperspectral WUE in BSR Disease Severity

The use of the WUE variable in conjunction with other leaf physiology metrics and hyperspectral wavelengths data represents a novel approach to forecasting plant stress conditions, particularly in terms of BSR disease severity, which has been relatively underexplored in previous research endeavours. Descriptive statistics for the training and validation model are revealed in Table 3.

Table 3
Result in descriptive statistics for training and validation model sample in WUE Modelling

Descriptive statistic for training model sample					
Variables	N	Minimum	Maximum	Mean	Std. Dev
E	18	.99	6.21	3.36	1.22
P_r	18	3.9	15.26	8.85	2.8
T_r	18	1.9	4.0	2.83	.50
TempL	18	28.34	31.4	29.9	.80
Ci	18	236.27	349	301	28.54
g_s	18	.00	.37	.16	.12
F	18	57.4	77.14	69.23	5.59
w717.4	18	.00	1.0	.51	.3
w736.7	18	.82	1.0	.9	.08
w741	18	.89	1.0	.93	.05
w790.8	18	.99	1.0	10	.00
w860.7	18	.82	1.0	.90	.08
E	6	2.05	4.64	3.4	1.14
P_r	6	2.24	16.92	8.33	4.99

T_r	6	2.15	3.69	2.72	.54
TempL	6	28.48	34.32	31.02	2.39
Ci	6	263.43	314.99	292.54	19.17
g_s	6	.07	.33	.20	.09
F	6	67.18	72.93	70.27	2.35
w717.4	6	.48	.57	.52	.4
w736.7	6	.82	.87	.84	.02
w741	6	.87	.92	.89	.02
w790.8	6	.99	.99	.99	.00
w860.7	6	.82	.87	.84	.02

Note: The variables unit included WUE (E) (µmol CO_2 H_2O $mmol^{-1}$); Photosynthetic Rate (P_r) (µmol m^{-2} s^{-1}); Transpiration Rate (T_r) (mol m^{-2} s^{-1}); Temperature Leaf (TempL) (°C); Intercellular CO_2 Concentration (Ci) (µmol mol^{-1}); Stomata Conductance (g_s) (mol m^{-2} s^{-1}); and Chlorophyll Content (F) (SPAD unit)

According to the model outcomes, only Ci, P_r, g_s, and w741 variables have substantive relevance in the model-building process, forcing the elimination of other variables (w860.7, w790.8, w717.4, w736.7, T_r, TempL and F) using the Stepwise Multiple Linear Regression model. The model summary provided in Table 4 further elucidates that four unique models have been determined, displaying commendable adjusted r-square values ranging from 76% to 95%, highlighting their efficacy in facilitating BSR disease.

Table 4
Empirical model derived from stepwise multiple linear regression model

No.	WUE Model Derived	R^2
1	WUE: 14.67 - 0.04 (Ci)	0.76
2	WUE: 9.24 - 0.03 (Ci) + 0.19 (P_r)	0.87
3	WUE: 9.53 - 0.03 (Ci) + 0.2 (P_r) -1.8 (g_s)	0.9
4	WUE: 19.85 - 0.02 (Ci) + 0.27 (P_r) -7.01 (g_s) - 14.02 (w741)	0.95

Based on Table 4, the initial model equation (Model 1) relies only on the Ci variable for model development, resulting in RMSE values for the training and validation model in 0.61 and 0.67 with (R^2:0.68, 0.83) respectively in Table 5.

Table 5
Summarizations result in accuracy assessment models generated

Model	Training Model RMSE	Validation Model RMSE	Training Model Regression Plot (R^2)	Validation Model Regression Plot (R^2)
1	0.61	0.67	0.68	0.83
2	0.44	0.35	0.83	0.98
3	0.39	0.35	0.88	0.97
4	0.44	0.37	0.92	0.98

While this represents a good predictive capacity, it is surpassed by later model iterations, in which the inclusion of new factors significantly improves forecast precision. For example, the introduction of the P_r variable in model 2 results in a significant drop for RMSE values for training and validation into 0.44, 0.35 with R^2:0.83,0.98.This result demonstrates the incremental gain in predictive accuracy. Model 3 extends this trend by incorporating another leaf physiology variable (g_s), resulting in an additional drop in RMSE values across both training and validation samples (0.39,0.35) with R^2:0.88, 0.97. The culmination of this iterative approach is seen in model 4, where the addition of a specific hyperspectral wavelength (w741) to the model equation adds to a slight decrease in RMSE values with 0.44, 0.37 with R^2:0.92,0.98 compared to its predecessor. Although the combination of data from different platforms may have a minor impact on prediction accuracy, the small difference in error magnitudes justifies the model's acceptance and use. In conclusion, the models can be ranked Model 1, Model 2, Model 4 and Model 3 in ascending order of accuracy based on RMSE values. The inclusion of hyperspectral wavelength (w741) in Model 4 is noteworthy as it enables more detailed studies, such as vegetation indices and geographical mapping forecasts, which expand the study's scope and granularity of results beyond the limitations of individual leaf physiological characteristics.

3.2 Analyse Mapping in WUE Hyperspectral Modelling in Oil Palm Plantation

Based on the previous result obtained in model WUE hyperspectral development, 4 maps of oil palm plantations have been generated to show an overview of WUE estimation in the study area in Figure 5.

Indications for healthy and stressed mature oil palms are revealed based on WUE value in the legend section on the map where WUE in 3.5 above is regarded as a healthy oil palm tree while less than that in stressed condition. Moreover, the colour tone presented in the map legend is shown from green to red in continuous display for their estimation severity changes in WUE. In the first assessment, all maps show consistency in terms of estimation WUE based on severity levels. As for healthy WUE in oil palm, most of the maps generated highlighted the centre of the maps with green and a combination of a little bit of yellow and orange colour. This reasons due to the sample existing in that area in healthy conditions (T0) affected with BSR disease (T1, T 2, T3). However, this scenario contradicts the right-hand side of the maps where domination estimation for WUE with red colour for seriously stressed oil palm. The sample that exists in the region shows that most of the sample numbers covered T1, T2 and T3 with a minimal number of healthy oil palm trees. This concludes that the chances for the BSR disease getting worse where the affected oil palm trees distance close to one or another is possible. This justification is supported by Mohd Shukri *et al.,* [23] where the potential for the BSR disease to spread from neighbouring palms through root-to-root contact. However, further investigation is required for this phase. In terms of visualization maps, the estimation WUE map generated from Model 4 shows a better map in visualizing real perspectives of oil palm trees on a plantation compared to Models 1, 2 and 3. The features of the crown tree appear in model 4 due to the combination of significant hyperspectral wavelength image (w741) as a supporting variable in model development. This result is different from the other maps as the rest solely depends on the leaf physiology as a variable in the model established. Therefore, it concludes that the addition of different data in model development improves the quality of the map generated as Adin *et al.,* [24], especially for estimation in WUE in oil palm plantations.

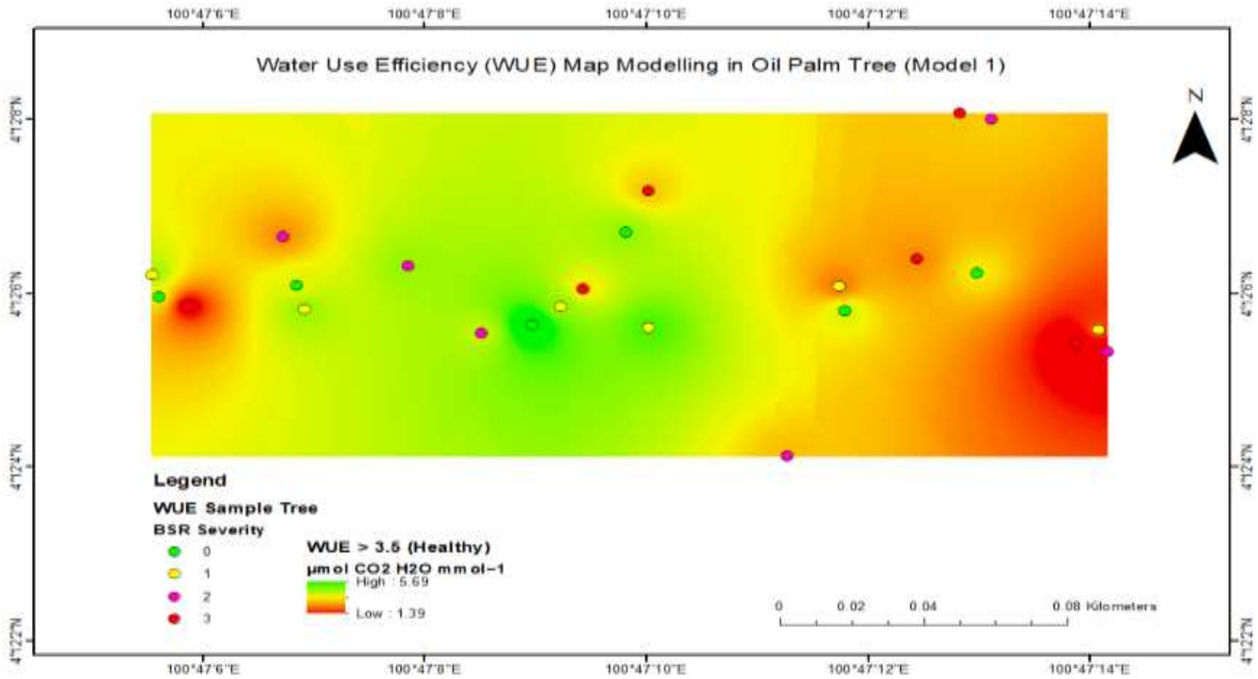
Water Use Efficiency (WUE) Map Modelling in Oil Palm Tree (Model 1)
Legend
WUE Sample Tree
BSR Severity
0
1
2
3
WUE > 3.5 (Healthy)
µmol CO2 H2O mmol−1
High : 5.69
Low : 1.39
0 0.02 0.04 0.08 Kilometers
N

(a)

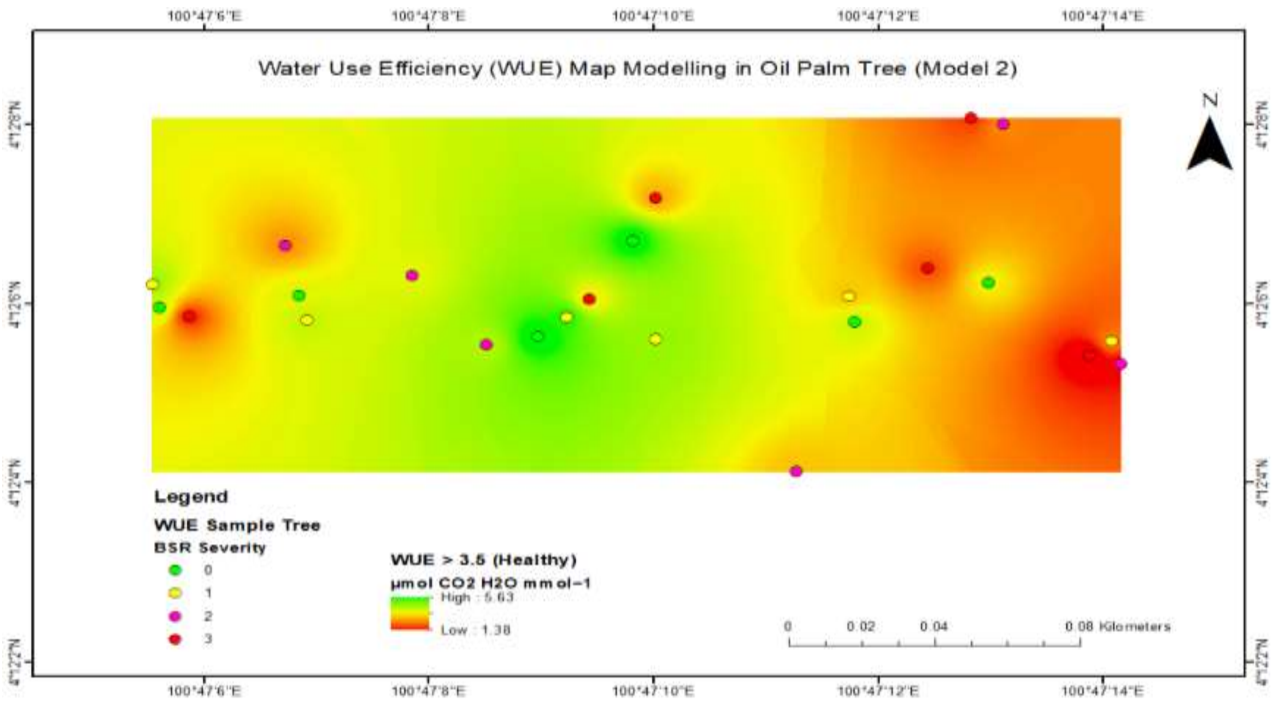
Water Use Efficiency (WUE) Map Modelling in Oil Palm Tree (Model 2)
Legend
WUE Sample Tree
BSR Severity
0
1
2
3
WUE > 3.5 (Healthy)
µmol CO2 H2O mmol−1
High : 5.63
Low : 1.38
0 0.02 0.04 0.08 Kilometers
N

(b)

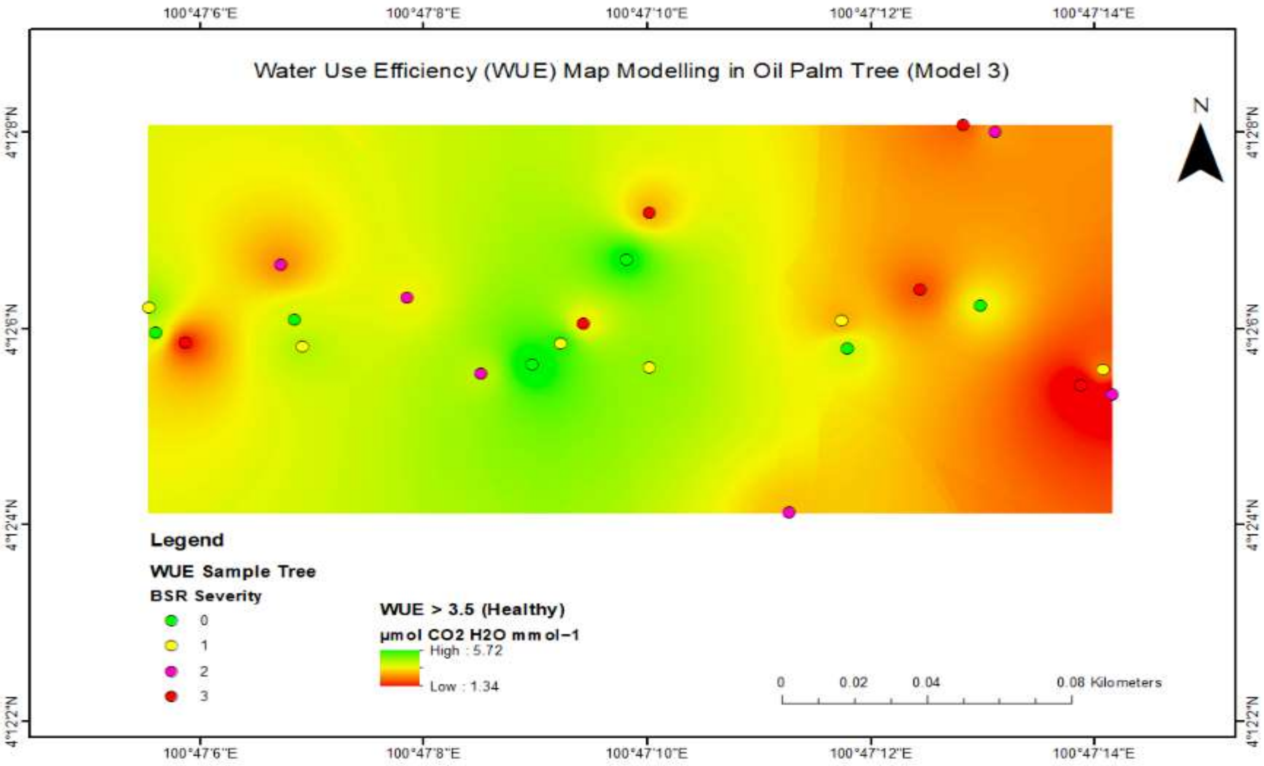

(c)

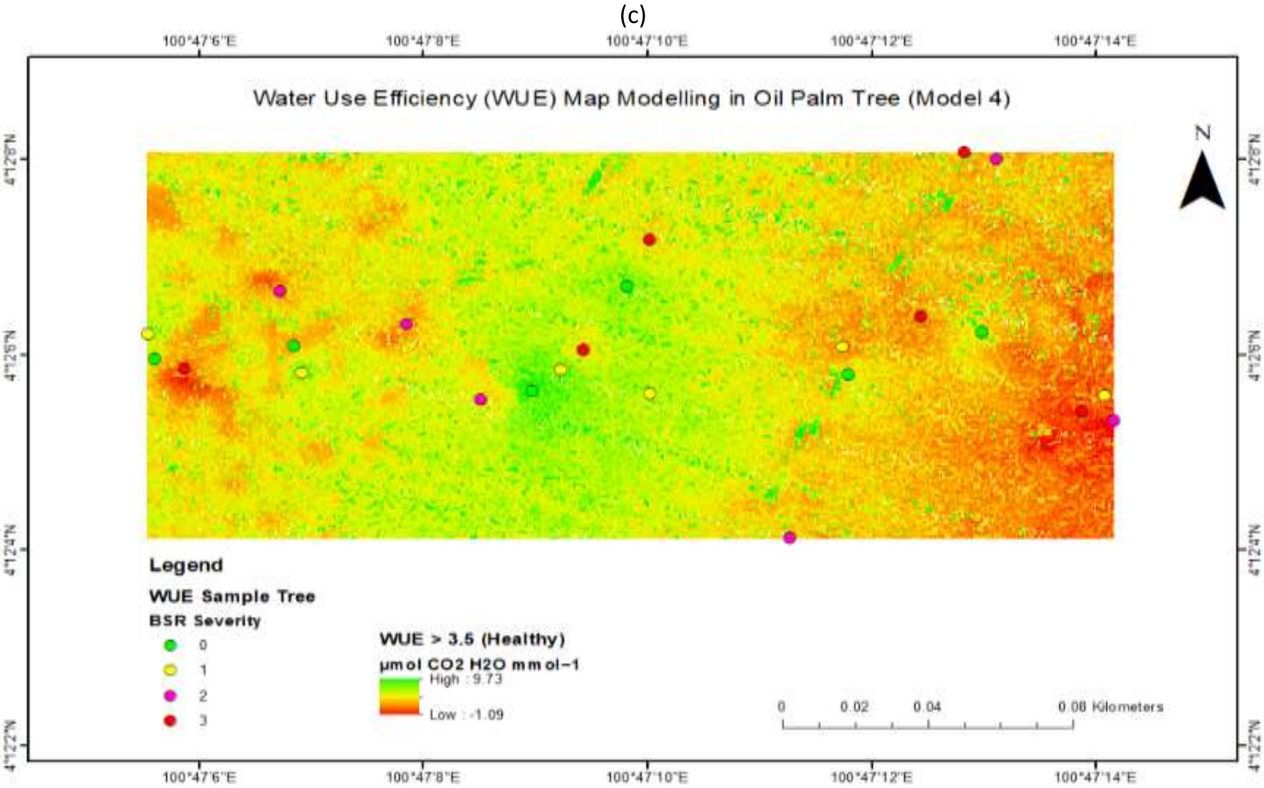

(d)

Fig. 5. Mapping oil palm plantation for WUE estimation based on a model developed. (a: Model 1, b: Model 2, c: Model 3, d: Model 4)

4. Conclusions

The study of Basal Stem Rot disease in oil palms is at the forefront of current research on oil palms as a reflection of growing concern since the disease affects oil palm cultivation at all growth phases, from seedling initiation to maturity. This pervasive danger significantly hampers the production of oil palm. The objectives of this research was to:

i. Propose a new novelty model in predicting plant stress with leaf physiology and hyperspectral data
ii. Analyse mapping for oil palm plantations.

Based on the result obtained, demonstrated 4 significant models were established (Model 1, Model 2, Model 3, Model 4) based on training and validation model samples in RMSE and regression plot value. Other than that, this study analyses the estimation of WUE in mapping for oil palm plantations where highlighting that the distance between healthy and affected BSR disease oil palm trees might influence the estimation for WUE, and details investigation is required in this part. Moreover, the additional variable from significant hyperspectral image (W741) can improve visualization in maps produced from the models.

Acknowledgement
The Ministry of Higher Education (MOHE), Malaysia, kindly provided financing for this research under the framework of the Fundamental Research Grant Scheme (FRGS) (Grant Nos.: FRGS/1/2021/WAB04/UITM/02/2 and 600-RMC/FRGS 5/3 (066/2021).

References
[1] Khosrokhani, Maryam, Siti Khairunniza-Bejo, and Biswajeet Pradhan. "Geospatial technologies for detection and monitoring of Ganoderma basal stem rot infection in oil palm plantations: a review on sensors and techniques." *Geocarto International* 33, no. 3 (2018): 260-276. https://doi.org/10.1080/10106049.2016.1243410
[2] Murphy, Denis J., Kirstie Goggin, and R. Russell M. Paterson. "Oil palm in the 2020s and beyond: challenges and solutions." *CABI agriculture and bioscience* 2 (2021): 1-22. https://doi.org/10.1186/s43170-021-00058-3
[3] Jazuli, Nur Aliyah, Assis Kamu, Khim Phin Chong, Darmesah Gabda, Affendy Hassan, Idris Abu Seman, and Chong Mun Ho. "A review of factors affecting Ganoderma basal stem rot disease progress in oil palm." *Plants* 11, no. 19 (2022): 2462. https://doi.org/10.3390/plants11192462
[4] Paterson, R. Russell M. "Ganoderma boninense disease of oil palm to significantly reduce production after 2050 in Sumatra if projected climate change occurs." *Microorganisms* 7, no. 1 (2019): 24. https://doi.org/10.3390/microorganisms7010024
[5] Zakaria, Latiffah. "Basal stem rot of oil palm: The pathogen, disease incidence, and control methods." *Plant Disease* 107, no. 3 (2023): 603-615. https://doi.org/10.1094/PDIS-02-22-0358-FE
[6] Siddiqui, Yasmeen, Arthy Surendran, R. Russell M. Paterson, Asgar Ali, and Khairulmazmi Ahmad. "Current strategies and perspectives in detection and control of basal stem rot of oil palm." *Saudi Journal of Biological Sciences* 28, no. 5 (2021): 2840-2849. https://doi.org/10.1016/j.sjbs.2021.02.016
[7] Baharim, Mohd Sharul Aikal, Nor Aizam Adnan, Fazly Amri Mohd, Ainon Nisa Othman, Haris Abdul Rahim, Mohamad Haris Abd Azis, Idris Abu Seman, Mohamad Anuar Izzuddin, Nur Amanina Shahabuddin, and Abd Aziz Nordiana. "A review of ganoderma Basal Stem Rot (BSR) disease detection and mapping using geospatial and advanced techniques." *Geocarto International* 37, no. 25 (2022): 8100-8126. https://doi.org/10.1080/10106049.2021.1993350
[8] Lai, Jie Hong, and Siti Aisyah Munirah Bohang. "Effectiveness of Tube Potential Reduction and Scan Range in Dose Reduction in Computed Tomography (CT): A Systematic Review." *Journal of Health and Quality of Life* 4, no. 1 (2024): 33-54. https://doi.org/10.37934/jhqol.4.1.3354

[9] Baharim, Mohd Sharul Aikal, Nor Aizam Adnan, Mohamad Izzuddin Anuar, Angelynna Lovelyn Laurence, and Abdullah Abdul Samat. "Relationship analysis between Ganoderma boninense-derived Basal Stem Rot disease severity with multiple leaf physiology parameters in mature oil palm tree responses toward water use efficiency (WUE)." *Journal of Plant Pathology* 106, no. 4 (2024): 1801-1816. https://doi.org/10.1007/s42161-024-01762-5

[10] A'fifah, A. R., And M. H. Haniff. "Impacts of wet and dry periods on leaf gas exchange, water use efficiency and carbon isotope discrimination in different oil palm materials." *Journal of Oil Palm Research* 30, no. 4 (2018): 693-701.

[11] Koyama, Kohei, and Shuhei Takemoto. "Morning reduction of photosynthetic capacity before midday depression." *Scientific Reports* 4, no. 1 (2014): 4389. https://doi.org/10.1038/srep04389

[12] Jardim, Ricardo, and F. Morgado-Dias. "Savitzky–Golay filtering as image noise reduction with sharp color reset." *Microprocessors and Microsystems* 74 (2020): 103006. https://doi.org/10.1016/j.micpro.2020.103006

[13] Li, Yu-hang, Xin Tan, Wei Zhang, Qing-bin Jiao, Yu-xing Xu, Hui Li, Yu-bo Zou, Lin Yang, and Yuan-peng Fang. "Research and application of several key techniques in hyperspectral image preprocessing." *Frontiers in Plant Science* 12 (2021): 627865. https://doi.org/10.3389/fpls.2021.627865

[14] Izzuddin, M. A., A. Hamzah, M. N. Nisfariza, A. S. Idris, A. Nor Aizam, BM Sharul Aikal, A. A. Nordiana, A. Mohd Najib, and I. Mohd Shukri. "Denoising of hyperspectral signal from drone for Ganoderma disease detection in oil palm." *International Journal of Geoinformatics* 19, no. 5 (2023): 55-60. https://doi.org/10.52939/ijg.v19i5.2659

[15] Husin, Nur A., Siti Khairunniza-Bejo, Ahmad F. Abdullah, Muhamad SM Kassim, Desa Ahmad, and Mohd HA Aziz. "Classification of basal stem rot disease in oil palm plantations using terrestrial laser scanning data and machine learning." *Agronomy* 10, no. 11 (2020): 1624. https://doi.org/10.3390/agronomy10111624

[16] Azmi, Aiman Nabilah Noor, Siti Khairunniza-Bejo, Mahirah Jahari, Farrah Melissa Muharram, and Ian Yule. "Identification of a suitable machine learning model for detection of asymptomatic Ganoderma boninense infection in oil palm seedlings using hyperspectral data." *Applied Sciences* 11, no. 24 (2021): 11798. https://doi.org/10.3390/app112411798

[17] Xie, Shanshan, Yan Zhang, Danjv Lv, Xu Chen, Jing Lu, and Jiang Liu. "A new improved maximal relevance and minimal redundancy method based on feature subset." *The Journal of supercomputing* 79, no. 3 (2023): 3157-3180. https://doi.org/10.1007/s11227-022-04763-2

[18] Azizan, Farah Liyana, Saratha Sathasivam, Muraly Velavan, Nur Rusyidah Azri, and Nur Iffah Rafhanah Abdul Manaf. "Prediction of drug concentration in human bloodstream using Adams-Bashforth-Moulton method." *Semarak Engineering Journal* 4, no. 1 (2024): 29-46. https://doi.org/10.37934/araset.29.2.5371

[19] Ali, Yasir, Ahmed Raza, Sidra Iqbal, Azhar Abbas Khan, Hafiz Muhammad Aatif, Zeshan Hassan, Ch Muhammad Shahid Hanif *et al.,* "Stepwise regression models-based prediction for leaf rust severity and yield loss in wheat." *Sustainability* 14, no. 21 (2022): 13893. https://doi.org/10.3390/su142113893

[20] Viertel, Philipp, and Matthias König. "Pattern recognition methodologies for pollen grain image classification: a survey." *Machine Vision and Applications* 33, no. 1 (2022): 18. https://doi.org/10.1007/s00138-021-01271-w

[21] Xing, Dong, Yulin Wang, Penghui Sun, Huahong Huang, and Erpei Lin. "A CNN-LSTM-att hybrid model for classification and evaluation of growth status under drought and heat stress in chinese fir (Cunninghamia lanceolata)." *Plant Methods* 19, no. 1 (2023): 66. https://doi.org/10.1186/s13007-023-01044-8

[22] Li, Zhanglin. "An enhanced dual IDW method for high-quality geospatial interpolation." *Scientific reports* 11, no. 1 (2021): 9903. https://doi.org/10.1038/s41598-021-89172-w

[23] Shukri, I. Mohd, M. A. Izzuddin, R. Mohd Hefni, and A. S. Idris. "Geostatistics of oil palm trees affected by Ganoderma disease in low and high planting density." In *IOP Conference Series: Earth and Environmental Science*, vol. 540, no. 1, p. 012065. IOP Publishing, 2020. https://doi.org/10.1088/1755-1315/540/1/012065

[24] Adin, Khaled Sharaf, Sharafaddin Saleh, and Bilkis Zabara. "The Quality of Stormwater in Sana'a City from the Perspective of Integrated Water Resources Management." *Journal of Advanced Research in Technology and Innovation Management* 3, no. 1 (2022): 1-10.